International Journal of Engineering Research and General ScienceVolume 2, Issue 5, August – September 2014
ISSN 2091-2730

Aerodynamic Characteristics of G16 Grid Fin Configuration at Subsonic and Supersonic Speeds

Prashanth H S[1], Prof. K S Ravi[2], Dr G B Krishnappa[3]

[1]M.Tech Student, Department of Mechanical Engineering, Vidyavardaka college of Engineering, Mysore, Karnataka

[2]Associate Professor, Department of Mechanical Engineering, Vidyavardaka college of Engineering, Mysore, Karnataka

[3] Professor and HOD, Department of Mechanical Engineering, Vidyavardaka college of Engineering, Mysore, Karnataka

e mail: hsprashanth63@gmail.com, Phone No: +91 9916886610

Abstract: Grid fins (lattice fins) are used as a lifting and control surface for highly maneuverable missiles in place of more conventional control surfaces, such as planar fins. Grid fins also find their applications for air-launched sub-munitions. The main advantages are its low hinge moment requirement and good high angle of attack performance characteristics. In this paper, one such grid fin configuration named G16 grid fin was taken for the CFD analysis. The G16 fin was studied under standalone condition at 0.7 & 2.5 Mach number for different Angle of attack (AOA) from 0 to 30° . The aerodynamic characteristics were plotted and discussed.

Keywords: Grid fins, Lift and Drag, Angle of Attack, ANSYS

I. INTRODUCTION

In a modern military, a missile is a self-propelled guided weapon system. Missiles have four system components: targeting and/or guidance, flight system, engine, and warhead. Missiles come in types adapted for different purposes: surface-to-surface and air-to-surface (ballistic, cruise, anti-ship, anti-tank), surface-to-air (anti-aircraft and antiballistic), air-to-air and anti-satellite missiles.

Grid fins (or lattice fins) [1] are a type of flight control surface used on missiles and bombs in place of more conventional control surfaces, such as planar fins. Grid fin looks much like a rectangular box filled with a lattice structure similar to a waffle iron or garden trellis. The grid is formed by small intersecting planar surfaces that create individual cells shaped like cubes or triangles. The box structure is inherently strong allowing the lattice walls to be very thin, reducing weight and the cost of materials.

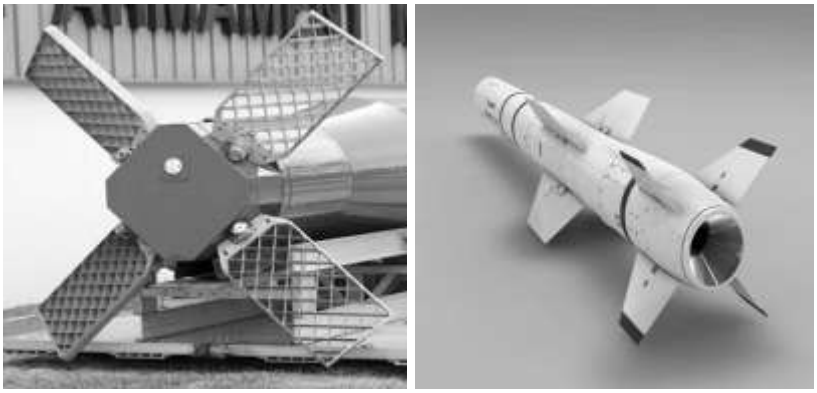

Figure 1.1: Grid Fins and Planar Fins

The primary advantage of grid fins is that they are much shorter than conventional planar fins in the direction of the flow. As a result, they generate much smaller hinge moments and require considerably smaller servos to deflect them in a high-speed flow [4]. The small chord length of grid fins also makes them less likely to stall at high angles of attack. This resistance to stall increases the control effectiveness of grid fins compared to conventional planar fins. Another important aerodynamic characteristic of grid fins concerns drag, although it can be an advantage or a disadvantage depending on the speed of the airflow.

In general, the thin shape of the lattice walls creates very little disturbance in the flow of air passing through, so drag is often no higher than a conventional fin. At low subsonic speeds, for example, grid fins perform comparably to a planar fin. Both the drag and control effectiveness of the lattice fin are about the same as a conventional fin in this speed regime.

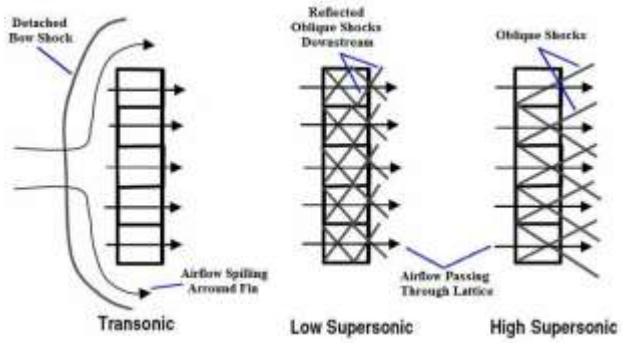

Figure 1.2: Flow over the grids at different flow regimes

The same behavior does not hold true at high subsonic numbers near Mach 1. Drag rises considerably higher and the fins become much less effective in this transonic region because of the formation of shock waves [2]. The flow behavior over the grid fins at various flow regimes are illustrated in Fig. 1.2.

II. G16 GRID FIN GEOMETRICAL DETAILS, MESH GENERTAION AND BOUNDARY CONDITIONS

The grid fin G16 geometry was taken from the previous existing experimental work [3]. Geometry was designed in CATIA V5 and Mesh was generated using ANSYS ICEM CFD 14.5. The simulations were carried out in the ANSYS CFX 14.5 solver.

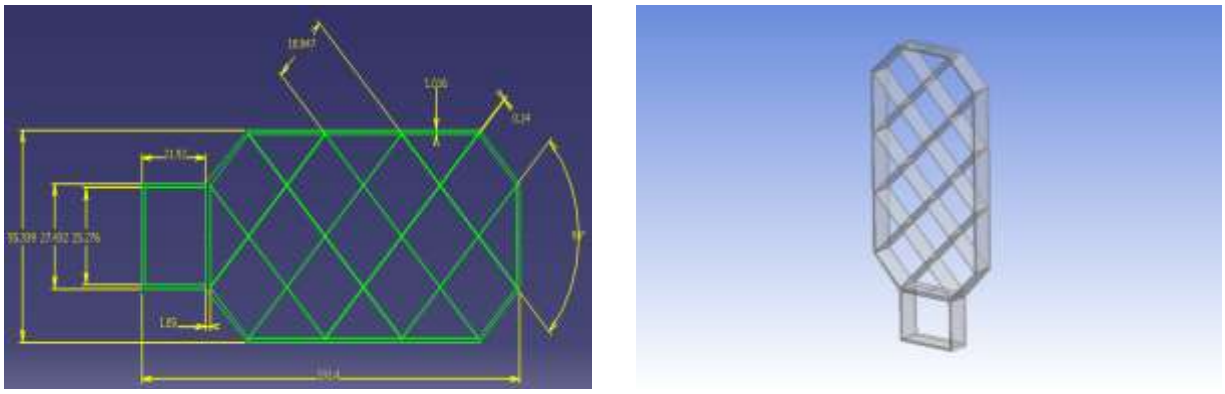

Figure 2.1: Geometric Details of G16 Fin (Dimensions are in mm) and Model created in CATIA V5 software

Wind tunnel like setup is provided by creating a fluid domain over the fin with suitable dimensions in the upstream and downstream directions. The whole body was imported to ANSYS workbench ICEM CFD 14.5 meshing tool and the unstructured Tetrahedral mesh (Fig. 2.2) is created. After a grid independence study a mesh with total of 2621519 elements and 495961 nodes were selected for the analysis. After the mesh, 4 inflation layers (Fig. 2.2) were applied over the surfaces of the fin with growth rate of 1.15 from the initial length. The insertion of inflation layers to the existing mesh helps to accurate capture of boundary effects near the proximities and curves of the body and also gives quicker results.

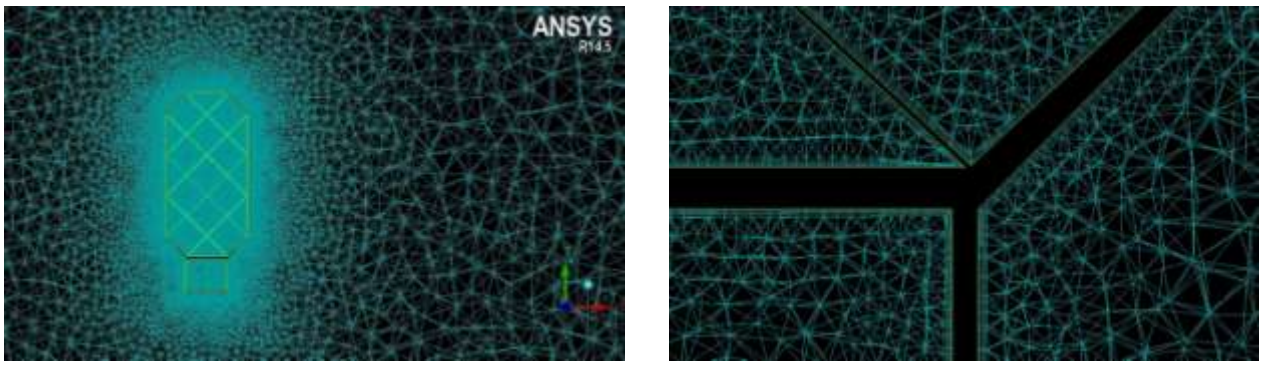

Figure 2.2: Cut plane showing unstructured mesh around Grid fin and Inflation layers over the surface of Grid fins

The imported G16 mesh data is analyzed in the ANSYS CFD code CFX 14.5 solver [5] for the 0.7 and 2.5 Mach Numbers for AOA 0, 5, 10, 15, 20, 25 and 30 degrees. The following boundary conditions were applied. Velocity inlet for Inlet, static pressure condition in the outlet, opening conditions for the domain walls and no-slip velocity for the fin surface.

For simulation, the k-ω based Shear Stress Transport (SST) turbulence model was selected. The SST the model accounts for the transport of the turbulent shear and gives highly accurate prediction of the onset and the amount of flow separation under adverse pressure gradients. Since the thermal problem was not of importance in the present study, option total energy was selected. Under the equation class settings the upwind advection scheme was selected for faster results output and the convergence criteria is set to residual type (RMS). The problem was setup for the standard atmospheric pressure conditions.

III. Results and Discussion

After the simulation achieved desired convergence criteria, the output results were analyzed in the post processor CFD POST 14.5. The behavior of Velocity and Pressure contours and the body forces (Axial and Normal) were note down for the Aerodynamic coefficients calculation. The graphs for the same were plotted.

Following figures show the pressure and velocity distribution over the grid fin for AOA 0◦ & 20◦ at 0.7 & 2.5 Mach numbers.

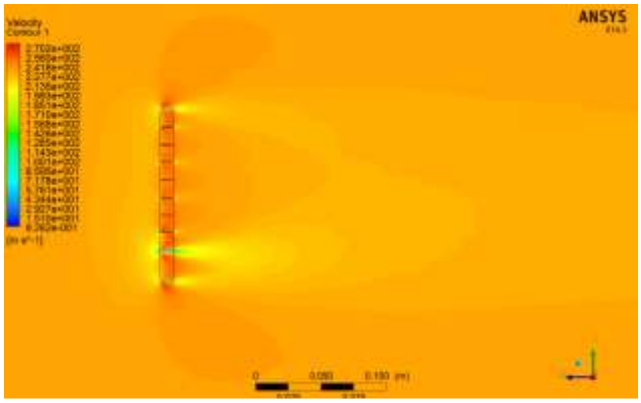

Figure 3.1: Velocity contour on a cut plane at Mach 0.7, AOA 0˚

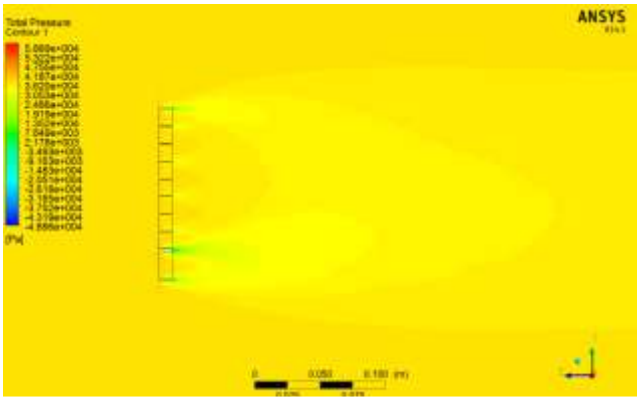

Figure 3.2: Pressure contour on a cut plane at Mach 0.7, AOA 0˚

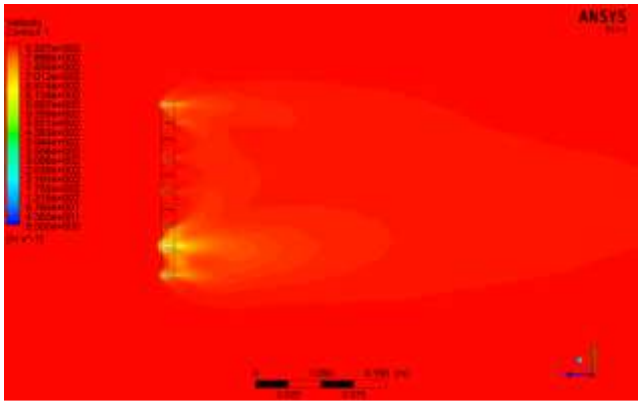

Figure 3.3: Velocity contour on a cut plane at Mach 2.5, AOA 0˚

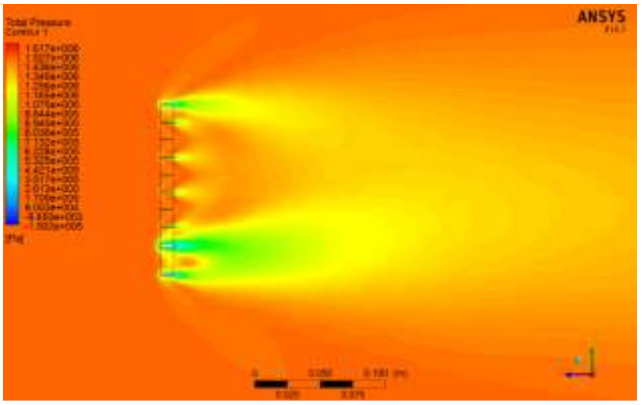

Figure 3.4: Pressure contour on a cut plane at Mach 2.5, AOA 0˚

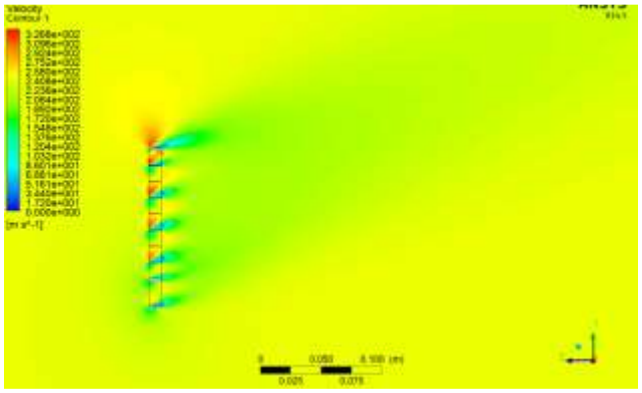

Figure 3.5: Velocity contour on a cut plane at Mach 0.7, AOA 30˚

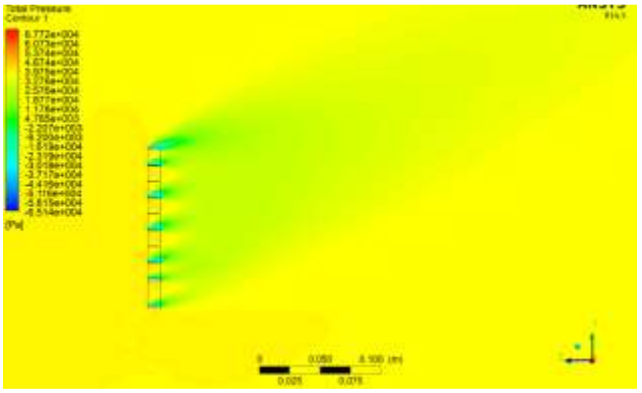

Figure 3.6: Pressure contour on a cut plane at Mach 0.7, AOA 30˚

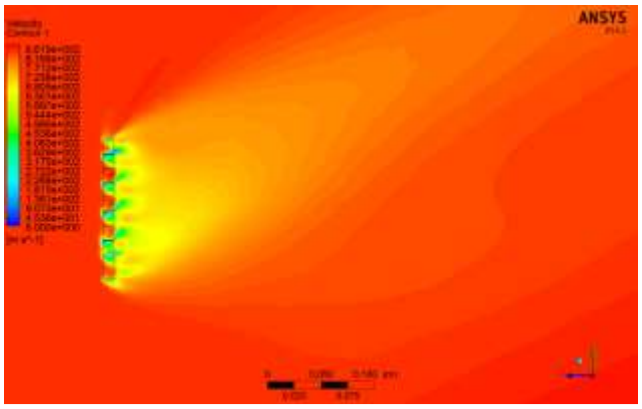

Figure 3.7: Velocity contour on a cut plane at Mach 2.5, AOA 30˚

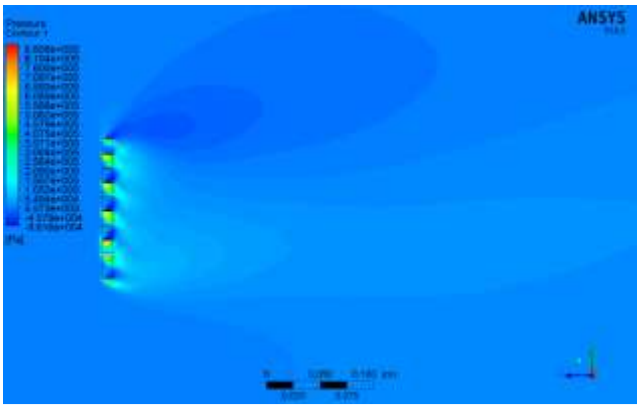

Figure 3.8: Pressure contour on a cut plane at Mach 2.5, AOA 30˚

Following Graphs shows the comparison between different aerodynamic characteristics against AOA for Mach 0.7 and Mach 2.5.

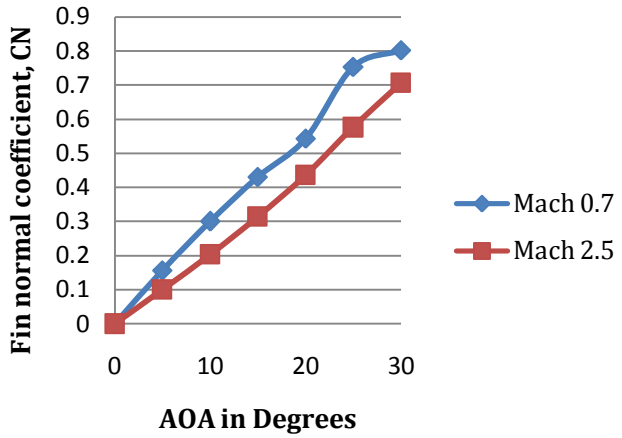

Figure 3.9: C_N v/s AOA for Mach 0.7 and Mach 2.5

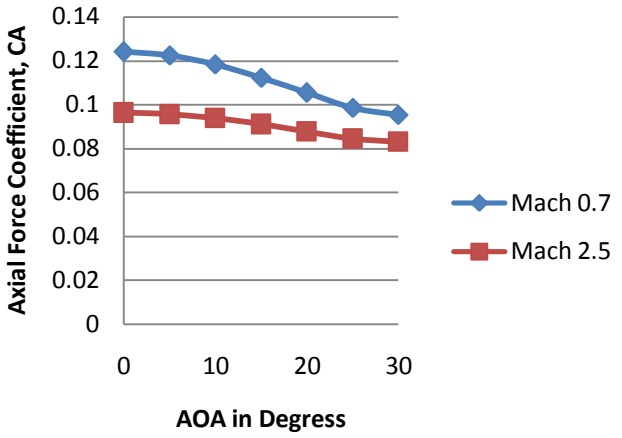

Figure 3.10: C_A v/s AOA for Mach 0.7 and Mach 2.5

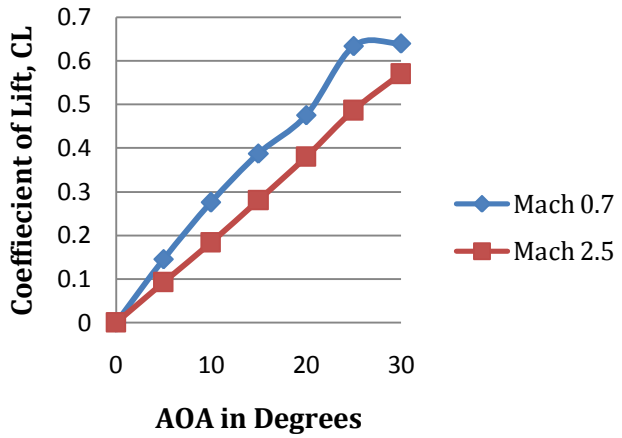

Figure 3.11: C_L v/s AOA for Mach 0.7 and Mach 2.5

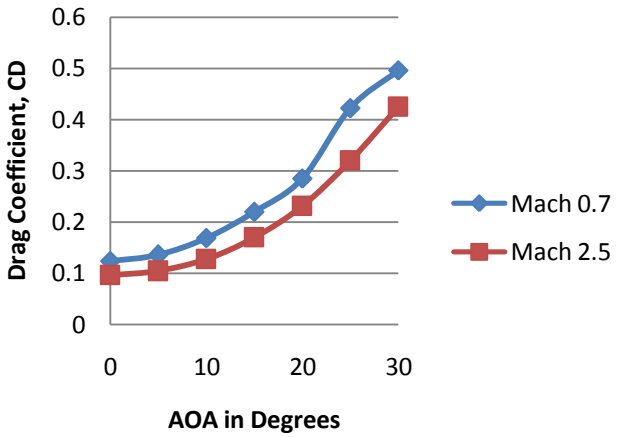

Figure 3.12: C_D v/s AOA for Mach 0.7 and Mach 2.5

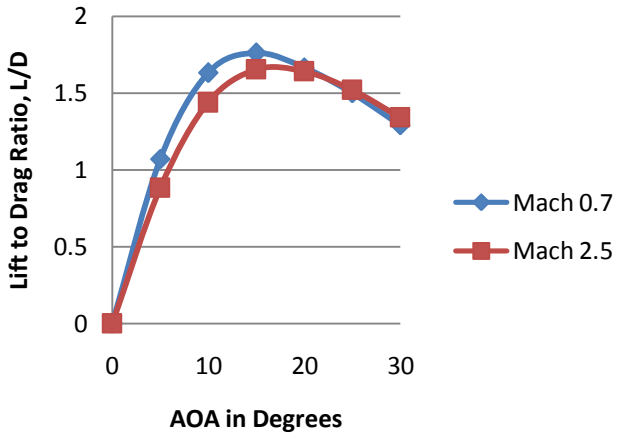

Figure 3.13: L/D v/s AOA for Mach 0.7 and Mach 2.5

Inference from the Graphs:

Figure 3.9 shows the graph of Normal force coefficient versus AOA for Mach 0.7 & 2.5. It is seen that C_N value for Mach 0.7 is greater than Mach 2.5 for all AOAs and the C_N for both Mach 0.7 & 2.5 increases as the AOA increases.

Figure 3.10 shows the graph of Axial Force coefficient versus AOA for Mach 0.7 and 2.5. It is that the C_A for the Mach 0.7 is slightly greater than Mach 2.5. For both Mach 0.7 and 2.5, the C_A value slightly decreases as the AOA increases.

Figure 3.11 shows the graph of Coefficient of Lift, C_L versus AOA for Mach 0.7 and Mach 2.5. It is seen the lift produced for Mach 0.7 is greater than the lift produced at Mach 2.5 for all AOAs and also the C_L varies linearly with the increase in AOA for both Mach 0.7 & 2.5, except for Mach 0.7 after AOA 20◦.

Figure 3.12 shows the graph of Coefficient of drag, C_D versus AOA for Mach 0.7 & 2.5. It is seen that the drag levels at Supersonic speeds i.e. at Mach 2.5 is considerably reduced compared to subsonic speeds. At higher speeds (supersonic), the drag tends to decrease due to the smaller oblique shock angle and the shock passes through the grid along the chord length without intersecting it. However, at low supersonic and subsonic speeds the oblique shocks reflects within the grids producing more drag force which in turn affects the speed of the moving object. This shows that, the fin performs better at supersonic speeds. However, lift force is considerably low at supersonic speeds compared to subsonic speeds.

Figure 3.13 shows the graph of Lift to Drag ratio, L/D versus AOA for Mach 0.7 & 2.5. It is seen that, the up to AOA 20◦, the L/D ratio is more for Mach 0.7 and beyond 20◦, the L/D ratio is more of Mach 2.5. Also it is observed that for both Mach 0.7 and 2.5, the maximum L/D ratio appears at 15◦ and then it decreases with increase in AOA for both subsonic and supersonic flow regimes.

IV. CONCLUSION

Numerical simulations were successful in predicting the flow behavior at different flow regimes with varying AOAs. The following inferences can be seen from the analysis.

1. For all AOAs, the normal force coefficient C_N, axial force coefficient C_A and lift coefficient C_L were comparably greater in subsonic flow than in supersonic flow. Also it is seen that, C_N & C_L characters shows increase in the value as the AOA increases. But, for C_A it is vice versa.
2. At supersonic speeds, the drag levels were decreased compared to subsonic flows. This is due to the smaller oblique shock angle at supersonic speeds and the shock passes through the grid along the chord length without intersecting it.
3. The L/D ratio shows that, the performance of G16 fin is better at subsonic speeds up to AOA 20°. At AOA beyond 20°, the fin show improved performance at supersonic speeds. Also, the maximum L/D ratio occurs at AOA 15° for both flow regimes i.e. at Mach 0.7 & 2.5.
4. Overall it is concluded that, the G16 fins shows better performance at higher AOA and at higher speeds since, reduction in drag levels at Mach 2.5. However, the lift is to be improve at supersonic speeds.

REFERENCES:

[1] Scott, Jeff, “Missile Grid Fins” and “Missile Control Systems”, URL:http://www.aerospaceweb.org/questions/weapons/.

[2] Zaloga, Steve (2000). The Scud and Other Russian Ballistic Missile Vehicles. New Territories, Hong Kong: Concord Publications Co.

[3] Washington, W. D., and Miller, M. S., “Experimental Investigations of Grid Fin Aerodynamics: A Synopsis of Nine Wind Tunnel and Three Flight Tests,” Proceedings of the NATO RTO Applied Vehicle Technology Panel Symposium on Missile Aerodynamics, RTO-MP-5, NATO Research and Technology Organization, Cedex, France, Nov. 1998.

[4] Salman Munawar., "Analysis of grid fins as efficient control surface in comparison to conventional planar fins," 27th International Congress of the Aeronautical Sciences, 2010.

[5] ANSYS 14.5 CFX, Help PDF: Solver Modeling Guide